The bone-sparing effects of estrogen and WNT16 are independent of each other

Sofia Movérare-Skrtic[a], Jianyao Wu[a], Petra Henning[a], Karin L. Gustafsson[a], Klara Sjögren[a], Sara H. Windahl[a], Antti Koskela[b], Juha Tuukkanen[b], Anna E. Börjesson[a,c], Marie K. Lagerquist[a], Ulf H. Lerner[a], Fu-Ping Zhang[d], Jan-Åke Gustafsson[e,1], Matti Poutanen[a,d], and Claes Ohlsson[a,1]

[a]Centre for Bone and Arthritis Research at Institute of Medicine, Sahlgrenska Academy at University of Gothenburg, SE-41345 Gothenburg, Sweden; [b]Unit of Cancer Research and Translational Medicine, MRC Oulu and Department of Anatomy and Cell Biology, University of Oulu, FI-90014 Oulu, Finland; [c]Rheumatology and Bone Diseases Unit, Centre for Genomic and Experimental Medicine, MRC Institute of Genetics and Molecular Medicine, Western General Hospital, University of Edinburgh, Edinburgh, EH4 2XU, United Kingdom; [d]Institute of Biomedicine, Turku Center for disease modeling, Department of Physiology, University of Turku, FI-20520 Turku, Finland; and [e]Department of Biology and Biochemistry, Center for Nuclear Receptors and Cell Signaling, University of Houston, Houston, TX 77204

Contributed by Jan-Åke Gustafsson, October 14, 2015 (sent for review October 8, 2015; reviewed by Subburaman Mohan and Kalervo Väänänen)

Wingless-type MMTV integration site family (WNT)16 is a key regulator of bone mass with high expression in cortical bone, and *Wnt16*$^{-/-}$ mice have reduced cortical bone mass. As *Wnt16* expression is enhanced by estradiol treatment, we hypothesized that the bone-sparing effect of estrogen in females is WNT16-dependent. This hypothesis was tested in mechanistic studies using two genetically modified mouse models with either constantly high osteoblastic *Wnt16* expression or no *Wnt16* expression. We developed a mouse model with osteoblast-specific *Wnt16* overexpression (*Obl-Wnt16*). These mice had several-fold elevated *Wnt16* expression in both trabecular and cortical bone compared with wild type (WT) mice. *Obl-Wnt16* mice displayed increased total body bone mineral density (BMD), surprisingly caused mainly by a substantial increase in trabecular bone mass, resulting in improved bone strength of vertebrae L_3. Ovariectomy (ovx) reduced the total body BMD and the trabecular bone mass to the same degree in *Obl-Wnt16* mice and WT mice, suggesting that the bone-sparing effect of estrogen is WNT16-independent. However, these bone parameters were similar in ovx *Obl-Wnt16* mice and sham operated WT mice. The role of WNT16 for the bone-sparing effect of estrogen was also evaluated in *Wnt16*$^{-/-}$ mice. Treatment with estradiol increased the trabecular and cortical bone mass to a similar extent in both *Wnt16*$^{-/-}$ and WT mice. In conclusion, the bone-sparing effects of estrogen and WNT16 are independent of each other. Furthermore, loss of endogenous WNT16 results specifically in cortical bone loss, whereas overexpression of WNT16 surprisingly increases mainly trabecular bone mass. WNT16-targeted therapies might be useful for treatment of postmenopausal trabecular bone loss.

WNT16 | estrogen | cortical bone | trabecular bone | transgenic mice

Both estrogen and wingless-type MMTV integration site family (WNT)16 are crucial regulators of bone mass in women (1–5). The bone-sparing effect of estrogen is primarily mediated via estrogen receptor-α (ERα) (6). Estrogen-deficiency leads to rapid bone loss and contributes significantly to the development of postmenopausal osteoporosis that can be prevented by estradiol treatment. However, this treatment is associated with side effects such as breast cancer and thromboembolism (7, 8).

The WNTs are a family of secreted glycoproteins that consists of 19 members in mammals, and which mediates autocrine and paracrine effects by binding to frizzled (Fzd) receptors and LDL-related protein 5/6 (LRP5/6) coreceptors (9). During the last decade, several lines of clinical and preclinical evidence have indicated that WNT signaling is critical in bone development and in the regulation of adult bone homeostasis (10–20) and modulation of WNT signaling has emerged as a promising strategy for increasing bone mass (21–23). Crosstalk and synergy between ERα signaling and the WNT pathways have been described (24–26). In the brain, estrogen signaling activates WNT by down-regulating dickkopf-1 (Dkk1), a WNT antagonist, to prevent neurodegeneration (27). In the uterus, estrogen prompts the canonical WNT signaling pathway in the uterine epithelium to induce uterine epithelial cell growth (28), and in breast cancer, ERα activation enhances cell growth via WNT signaling (29).

Human genetic studies followed by subsequent mechanistic studies have recently revealed that WNT16 is a key physiological regulator of cortical bone mass and nonvertebral fracture risk (4, 5, 30–33). We recently demonstrated that WNT16 is osteoblast-derived and inhibits osteoclastogenesis both directly by acting on osteoclast progenitors and indirectly by increasing expression of osteoprotegerin (*Opg*) in osteoblasts (3). WNT16 is highly expressed in cortical bone but, for unknown reasons, only moderately expressed in trabecular bone. Experiments using WNT16-deleted mouse models clearly show that absence of WNT16 results in reduced cortical but not trabecular bone mass (3, 4, 30, 34). However, the effects of pharmacologically increased WNT16 levels on the cortical and trabecular bone compartments are unexplored. Furthermore, the role of WNT16 for the bone-sparing effect of estrogen is unknown. Herein we first demonstrate that the expression of WNT16 is enhanced by estradiol treatment, and we therefore hypothesized that the bone-sparing

Significance

Previous studies demonstrate that endogenous wingless-type MMTV integration site family (WNT)16 is a crucial regulator of cortical bone mass. Surprisingly, we demonstrate that overexpression of WNT16 increases mainly trabecular bone mass. Both estrogen and WNT16 are crucial regulators of bone mass, but the possible interaction between WNT16-signaling and estrogen-signaling is unknown. To determine the possible interaction between WNT16 and estrogen signaling in bone, we developed and used two genetically modified mouse models with either constantly high osteoblastic *Wnt16* expression or no *Wnt16* expression. We demonstrated that the bone-sparing effects of estrogen and WNT16 are independent of each other. As WNT16 signaling in bone does not require normal estrogen action, we propose that WNT16-targeted therapies might be useful for treatment of postmenopausal trabecular bone loss.

Author contributions: S.M.-S., J.-Å.G., and C.O. designed research; S.M.-S., J.W., P.H., K.L.G., K.S., S.H.W., A.K., J.T., A.E.B., and M.K.L. performed research; F.-P.Z. and M.P. contributed new reagents/analytic tools; S.M.-S., U.H.L., J.-Å.G., and C.O. analyzed data; and S.M.-S., J.-Å.G., and C.O. wrote the paper.

Reviewers: S.M., VA Loma Linda Healthcare System; and K.V., University of Turku.

The authors declare no conflict of interest.

[1]To whom correspondence may be addressed. Email: jgustafsson@uh.edu or Claes.Ohlsson@medic.gu.se.

This article contains supporting information online at www.pnas.org/lookup/suppl/doi:10.1073/pnas.1520408112/-/DCSupplemental.

effects of estrogen are WNT16-mediated. This hypothesis was tested in mechanistic studies using two different genetically modified mouse models in which estrogen does not have the capacity to regulate WNT16 levels. Contradicting our hypothesis, we demonstrate that the bone-sparing effects of estrogen and WNT16 are independent of each other. In addition, unexpectedly, we demonstrate that overexpression of WNT16 increases mainly trabecular bone mass.

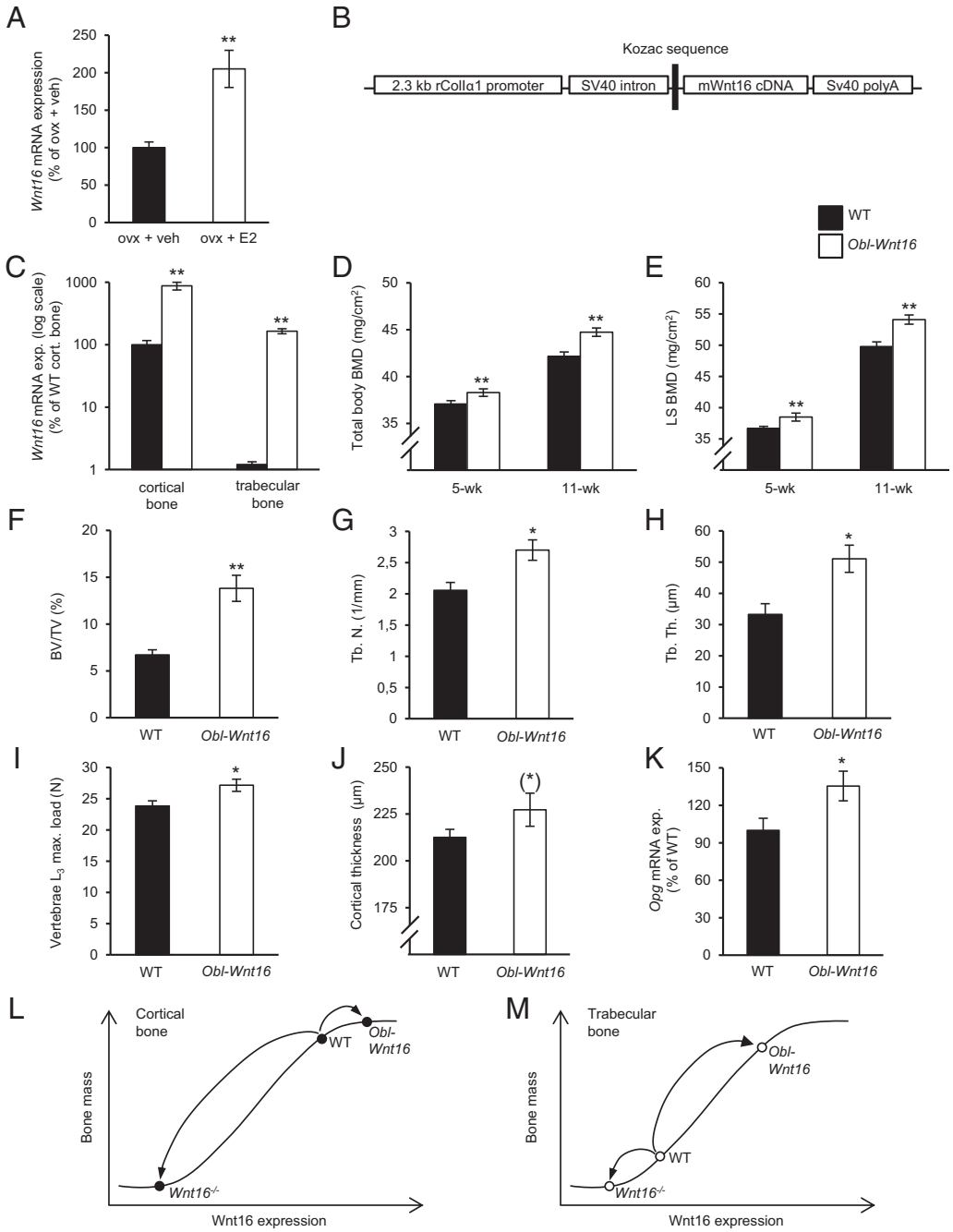

Fig. 1. Overexpression of *Wnt16* in osteoblasts substantially increases trabecular bone mass. (*A*) *Wnt16* mRNA expression in humerus of 16-wk-old ovariectomized wild-type (WT) mice after 4 wk of estradiol (E2, 167 ng/mouse/d) or vehicle (veh) treatment. $^{**}P < 0.01$; vs. ovx + veh using Student's *t* test. (*B*) Structure of the transgene used to overexpress the mouse *Wnt16* cDNA in the osteoblasts under the control of a 2.3-kb fragment of the rat Col-Iα1 promoter (*Obl-Wnt16* mice). (C) Bone-specific overexpression of *Wnt16* mRNA in 16-wk-old female *Obl-Wnt16* mice compared with WT mice ($n = 8$). (*D* and *E*) Total body (*D*) and lumbar spine (LS; *E*) bone mineral density (BMD) as measured by DXA in 5- and 11-wk-old female *Obl-Wnt16* mice and WT mice (n = 15–16). (*F–H*) Bone volume per total volume (BV/TV; *F*), trabecular number (Tb.N; *G*), and trabecular thickness (Tb.Th; *H*) of the distal metaphyseal region of femur in 16-wk-old female *Obl-Wnt16* mice and WT mice as measured by histomorphometry ($n = 8$). (*I*) Maximal load at failure of compression test of L_3 vertebrae of 16-wk-old female *Obl-Wnt16* mice and WT mice (n = 15–19). (*J*) Cortical thickness of femur of 16-wk-old female *Obl-Wnt16* mice and WT mice as measured by histomorphometry ($^{*}P = 0.17$, $n = 8$). (*K*) Osteoprotegerin (*Opg*) mRNA expression in the trabecular bone of 16-wk-old female *Obl-Wnt16* mice and WT mice as measured by real-time PCR. All values are given as mean ± SEM (*C–K*) $^{**}P < 0.01$, $^{*}P < 0.05$, Student's *t* test compared with WT. (*L–M*) Proposed dose–response curve between *Wnt16* expression and bone mass in cortical and trabecular bone, respectively.

Results

Overexpression of *Wnt16* in Osteoblasts Substantially Increases Trabecular Bone Mass. We initially observed that *Wnt16* expression in bone is enhanced by estradiol treatment in ovx female mice (Fig. 1*A*) and, therefore, we hypothesized that the bone-sparing effects of estrogen are WNT16-dependent. We first aimed to test this hypothesis in a mouse model with constant high *Wnt16* levels in bone. To this end we developed a transgenic mouse model (*Obl-Wnt16*) with osteoblast-specific *Wnt16* overexpression under the control of a 2.3-kb fragment of the rat type I α 1 procollagen promoter (Fig. 1 *B–K* and Tables S1–S4). The *Obl-Wnt16* mice displayed a specific and high overexpression of *Wnt16* in bone (Fig. 1*C*). The endogenous moderate *Wnt16* expression in trabecular bone was elevated 140-fold ($P < 0.01$), whereas the endogenous high *Wnt16* expression in cortical bone was increased 9-fold ($P < 0.01$) in *Obl-Wnt16* mice compared with WT mice, but still the *Wnt16* expression was higher in cortical bone than in trabecular bone in *Obl-Wnt16* mice (Fig. 1*C*). There was no change in *Wnt16* expression in the uterus in the *Obl-Wnt16* mice compared with WT mice ($P = 0.3$). The *Obl-Wnt16* mice were born at a normal Mendelian distribution, were apparently healthy and had unaffected tibia length, body weight and weights of several visceral organs compared with WT mice (Fig. 2*A* and Table S1).

DXA analysis revealed that the *Obl-Wnt16* mice had increased total body and lumbar spine (LS) BMD compared with WT mice both before (5-wk-old) and after (11- and 16-wk-old) sexual maturation ($P < 0.05$; Figs. 1 *D* and *E* and 2*B*). The trabecular and cortical bone compartments were analyzed separately at 16 wk of age using high-resolution μCT and histomorphometry. The trabecular bone volume fraction (BV/TV) was substantially increased (+106%, $P < 0.01$) in the distal metaphyseal region of femur in *Obl-Wnt16* mice compared with WT mice and this was the result of both increased trabecular number and thickness (Fig. 1 *F–H*). The trabecular BV/TV was also increased in the vertebrae of *Obl-Wnt16* mice (Fig. 2*C*). To evaluate whether the increased trabecular bone mass in *Obl-Wnt16* mice resulted in increased bone strength, L_3 vertebra was evaluated using a compression test, demonstrating that the maximal load at failure was significantly increased in *Obl-Wnt16* mice compared with WT mice (Fig. 1*I*). In contrast, there was only a nonsignificant tendency of increased cortical bone thickness in *Obl-Wnt16* mice compared with control mice (+6.9%, $P = 0.17$; Fig. 1*J*). Surprisingly, this demonstrates that overexpression of *Wnt16* in osteoblasts increases bone mass mainly as a result of substantially increased trabecular bone mass.

The mRNA level of the anti-osteoclastogenic factor *Opg* was increased in the vertebral body of vertebrae L_6, which is a bone with relatively high trabecular bone content, in *Obl-Wnt16* mice compared with control mice ($P < 0.05$, Fig. 1*K*). However, no consistent significant effect on bone formation or bone resorption was observed in *Obl-Wnt16* mice compared with WT mice when

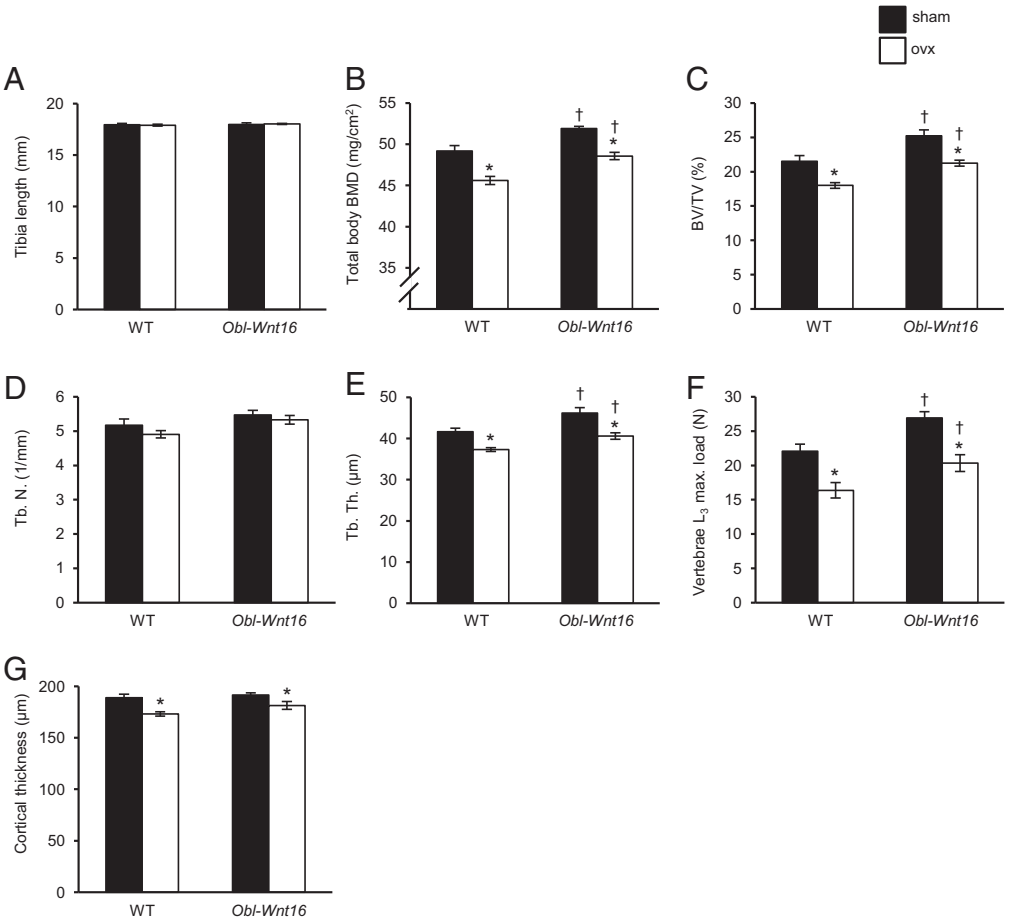

Fig. 2. The bone-sparing effects of estrogen and WNT16 are mediated via independent mechanisms, as evaluated in the *Obl-Wnt16* mouse model. (*A* and *B*) Tibia length (*A*) and total body bone mineral density (BMD; *B*) as measured by DXA. (*C–E*) Bone volume per total volume (BV/TV; *C*), trabecular number (Tb.N; *D*), and trabecular thickness (Tb.Th; *E*) of vertebrae L_4 as measured by micro-CT. (*F* and *G*) Maximal load at failure of compression test of L_3 vertebrae (*F*) and cortical thickness of femur (*G*), of 16-wk-old ovariectomized (ovx) female *Obl-Wnt16* mice and wild-type (WT) mice compared with sham mice ($n = 7–8$). Values are given as mean ± SEM $^*P < 0.05$ vs. sham; $^\dagger P < 0.05$ vs. WT using Student's *t* test.

bone turnover was evaluated in thorough studies using (*i*) static histomorphometry of osteoclast number in trabecular bone of the distal femur metaphysis and vertebrae L_5 (Table S2), (*ii*) dynamic histomorphometry of the trabecular bone in the distal femur metaphysis and vertebrae L_5 (Table S2), and the cortical bone of the middiaphyseal region of femur (Table S3), and (*iii*) biochemical serum bone marker analyses (Table S4; osteocalcin, type I collagen fragments, tartrate-resistant acid phosphatase 5b). These findings suggest that, although adult WNT16 transgenic mice have substantially increased trabecular bone mass, a new steady state of normal bone turnover has been reached in the trabecular bone.

The Bone-Sparing Effects of Estrogen and WNT16 Are Independent of Each Other When Evaluated in the *Obl-Wnt16* Mouse Model. We next used the *Obl-Wnt16* mouse model to test our hypothesis that the bone-sparing effect of estrogen is WNT16-dependent in female mice. This mouse model has a constant high *Wnt16* expression in bone. Twelve-week-old *Obl-Wnt16* and WT mice were ovx or sham-operated. Four weeks after ovx, the total body BMD, trabecular BV/TV, trabecular thickness, vertebral compression bone strength, and cortical bone thickness were reduced significantly and to a similar extent in ovx *Obl-Wnt16* and ovx WT mice compared with corresponding sham-operated mice (Fig. 2 *B–G*). This finding suggests that the bone-sparing effects of estrogens are not mediated via WNT16. In addition, the total body BMD, trabecular BV/TV, trabecular thickness, and vertebral compression bone strength were higher in the ovx *Obl-Wnt16* mice compared with ovx WT mice, demonstrating that the pharmacological stimulation by elevated *Wnt16* level on bone mass does not require estrogen action (Fig. 2 *B–F*). Notably, the total body BMD, trabecular bone volume fraction, trabecular bone thickness, and vertebral compression bone strength were similar in ovx *Obl-Wnt16* mice and sham-operated WT mice, implying that WNT16 overexpression could restore these bone parameters in ovx mice (Fig. 2 *B–F*). Jointly, these findings demonstrate that the bone-sparing effect of estrogen and WNT16 are independent of each other.

The Stimulatory Effect of Estrogen on Bone Does Not Require WNT16 When Evaluated in the *Wnt16*$^{-/-}$ Mouse Model. The role of WNT16 for the bone-sparing effect of estrogen was also evaluated in *Wnt16*$^{-/-}$ mice. In agreement with our previous observation (3), female *Wnt16*$^{-/-}$ mice had reduced cortical bone thickness (Fig. 3*A*), whereas the tibia length and trabecular bone mass was unaffected (Fig. 3 *B–E*) compared with WT mice. As adult *Wnt16*$^{-/-}$ mice develop spontaneous tibia fractures (3), we could not, due to ethical reasons, evaluate the potential effect of ovx on the bone strength in this mouse model. Instead, we treated female gonadal intact 4-wk-old WT and *Wnt16*$^{-/-}$ mice with a slightly supraphysiological dose of estradiol for four weeks, to further test if the stimulatory effect of estrogen on bone mass is dependent on WNT16. Estradiol treatment increased the trabecular BV/TV (Fig. 3*C*) as a result of increased trabecular number (Fig. 3*D*) both in WT and *Wnt16*$^{-/-}$ mice. In a similar manner, the cortical bone thickness in the middiaphyseal region of tibia was increased by estradiol treatment both in WT and *Wnt16*$^{-/-}$ mice (Fig. 3*A*). Thus, the effect of estradiol on bone does not require WNT16.

Discussion

Although it was recently established that endogenous osteoblast-derived WNT16 is a crucial regulator of cortical bone mass and that the WNT16 locus associates with nonvertebral fracture susceptibility, the interaction and crosstalk between WNT16 signaling and other major regulators of bone mass is essentially unknown (3–5, 30, 34). To determine the possible interaction between WNT16 and estrogen signaling in bone, we developed and used two genetically modified mouse models with either constantly high osteoblastic *Wnt16* expression or with no *Wnt16* expression. We demonstrated that the bone-sparing effects of estrogen and WNT16 are independent of each other. In addition, overexpression of WNT16 unexpectedly increased mainly trabecular bone mass.

To evaluate the interaction between estrogen action and WNT16 signaling in bone, we first developed a transgenic mouse model with osteoblast-specific *Wnt16* overexpression. Endogenous WNT16 is highly expressed in cortical bone but for unknown reasons only moderately expressed in trabecular bone (3). As we used an osteoblast-specific promoter, the overexpression of *Wnt16* in the *Obl-Wnt16* mouse model was bone-specific with several-fold increase of *Wnt16* levels in both the trabecular and cortical bone. Indeed, *Wnt16* levels in the trabecular bone of *Obl-Wnt16* mice were significantly higher than in the cortical bone of WT mice. *Obl-Wnt16*

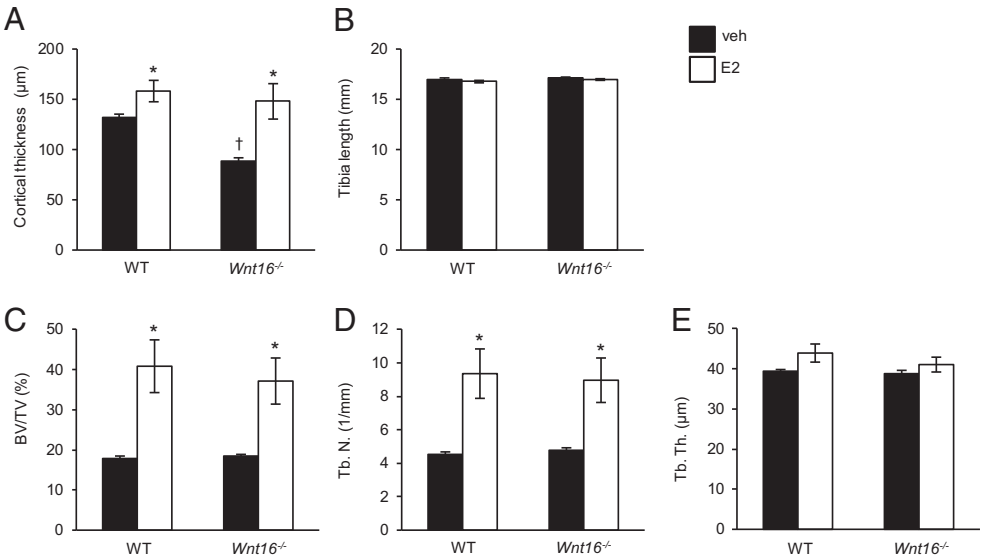

Fig. 3. The stimulatory effect of estrogen on bone does not require WNT16 as evaluated in the *Wnt16*$^{-/-}$ mouse model. Cortical thickness (*A*), tibia length (*B*), bone volume/total volume (BV/TV; *C*), trabecular number (Tb.N; *D*), and trabecular thickness (Tb.Th; *E*) as measured by micro-CT of 8-wk-old female *Wnt16*$^{-/-}$ or wild-type (WT) mice treated for 4 wk with estradiol (E2) or vehicle (veh) (n = 5–6). Values are given as mean ± SEM *P < 0.05 vs. veh using Student's t test.

mice were apparently healthy but had increased total body BMD that was mainly caused by a prominent increase in trabecular bone mass both in the metaphyseal region of the long bones and in the vertebrae. These changes were further associated with improved compression strength of the vertebrae. In contrast to observations in the trabecular bone, *Obl-Wnt16* mice displayed only a nonsignificant tendency for increased cortical bone mass. The unexpected finding that *Wnt16* overexpression in osteoblasts results in an effect mainly in the trabecular bone is in sharp contrast to the specific reduction of cortical bone mass described in previous mouse models with either global or osteoblast specific inactivation of *Wnt16* expression as well as the strong association observed between the *Wnt16* locus and cortical bone thickness in human genetic studies (3, 4). Based on these data, we propose that the high endogenous expression of WNT16 in cortical bone of WT mice results in a cortical bone mass value in the upper end of a sigmoidal dose–response curve between WNT16 expression and bone mass, with a substantial loss of cortical bone mass in the absence of WNT16 ($Wnt16^{-/-}$ mice), whereas overexpression of WNT16 (*Obl-Wnt16* mice) does not result in any major increase in cortical bone mass (Fig. 1*L*). In contrast, the relatively modest endogenous WNT16 expression in trabecular bone of WT mice results in a trabecular bone mass value that is at the lower end of this sigmoidal WNT16 dose–response curve. Thus, no major trabecular bone loss is observed in the absence of WNT16 (3), whereas overexpression of WNT16 markedly increases trabecular bone mass, as observed in the present study (Fig. 1*M*). These findings emphasize that pharmacological and physiological effects often differ, and we propose that enhancement of WNT16 signaling by pharmacological means would be useful for the treatment of trabecular bone loss. As we observed bone-site specific effects of WNT16, it is likely that osteoblast-derived WNT16, in a similar manner as observed for several other WNT proteins, acts as a short-range local cellular signal (35). This notion is further supported by the fact that WNT proteins are highly hydrophobic (36).

We have previously shown that osteoblast-derived WNT16 inhibits osteoclastogenesis, both directly and indirectly via increased production of *Opg* (3). This is supported by the reduced *Opg* levels in the $Wnt16^{-/-}$ mice. In the present study, the *Obl-Wnt16* mice had increased *Opg* mRNA levels in trabecular bone, indicating that elevated *Opg* levels might have contributed to the increased trabecular bone mass. However, no significant alterations of bone resorption or bone formation markers were observed in the *Obl-Wnt16* mice, suggesting that although adult WNT16 transgenic mice have substantially increased trabecular bone mass, a new steady state for the bone turnover has been reached.

Postmenopausal osteoporosis is caused by a pronounced drop in estrogen levels and ovariectomy of rodents has been widely used as an animal model of this disease (37, 38). Both estrogen and WNT16 are major regulators of bone mass (1–5), and in the first phase of the present study we demonstrated that estradiol treatment increases *Wnt16* expression in bone of ovx mice. We, thus, hypothesized that the bone-sparing effects of estrogens in females could be WNT16-dependent. The hypothesis was first evaluated using our *Obl-Wnt16* mouse model with constant several-fold increased *Wnt16* expression in both trabecular and cortical bone. However, ovariectomy reduced the trabecular and cortical bone mass similarly in *Obl-Wnt16* mice and WT mice, suggesting that the bone-sparing effects of estrogen are WNT16-independent. Conversely, total body BMD and trabecular bone mass were higher in the ovx *Obl-Wnt16* mice compared with ovx WT mice, demonstrating that the stimulatory effects of WNT16-overexpression on bone mass do not require estrogen action. All together, these data establish that the bone-sparing effects of estrogen and WNT16 act via independent mechanisms. Notably, the total body BMD and trabecular bone mass were similar in ovx *Obl-Wnt16* mice and sham operated WT mice, implying that WNT16 overexpression restores trabecular bone mass in ovx mice.

To further evaluate the interaction between the stimulatory effects of estrogen and WNT16 on bone mass, the role of WNT16 for the bone-sparing effects of estrogen was evaluated in $Wnt16^{-/-}$ mice. Estradiol treatment increased trabecular and cortical bone mass in both $Wnt16^{-/-}$ and WT mice, clearly demonstrating that the stimulatory effect of estrogen on bone mass does not require WNT16 expression.

In conclusion, using two different mouse models, we here demonstrate that, although WNT16 expression is stimulated by estrogen, the bone-sparing effect of estrogen and WNT16 are independent of each other. In addition, loss of endogenous WNT16 results specifically in cortical bone loss, whereas pharmacological overexpression of WNT16, surprisingly, increases mainly trabecular bone mass. As WNT16 signaling in bone does not require normal estrogen action, we propose that WNT16-targeted therapies might be useful for treatment of postmenopausal trabecular bone loss.

Materials and Methods

Development of an *Obl-Wnt16* Transgenic Mouse Line. To develop an osteoblast-specific WNT16 overexpressing mouse model (*Obl-Wnt16*), we generated a 4843 bp-long transgenic construct in pGL3 plasmid backbone. The transgene consists of the rat procollagen type I α 1 promoter (2.3 kb in length), simian virus 40 small-t intron as well as a full-length cDNA from mouse *Wnt16* and a SV40 polyA signal (Fig. 1*B*). For microinjection, the construct was linearized and cleaved from the plasmid backbone by restriction enzyme digestion using NotI and BamHI. Transgenic mouse lines were generated in the C57BL/6 genetic background by microinjecting the DNA into pronuclei of fertilized oocytes using standard techniques. Integration of the transgene was verified by PCR screening using DNA isolated from tissue biopsies obtained during ear marking of the potential founder mice, and of the offspring thereafter. The 5′-AGGAGGCACACGGAGTGAGG-3′ and 5′-CTGCTCCCATTCATCAGTTC-3′ primers were used for genotyping of the *Obl-Wnt16* mice.

Establishment of an *Obl-Wnt16* Transgenic Mouse Line. *Obl-Wnt16* mice showed normal fertility. All experiments were carried out on mice born from crossing a male *Obl-Wnt16* mouse with a female C57BL/6N mouse. WT littermates were used as control groups. The mice were fed standard phytoestrogen-free pellet diet ad libitum (R70, Lactamin AB). Ovariectomy (ovx) or sham operation were performed on 12-wk-old female mice and the mice were killed after 4 wk.

Mice with Total Inactivation of Wnt16. The generation of $Wnt16^{-/-}$ mice has been described (3). Four-week-old female $Wnt16^{-/-}$ and WT littermate mice were treated with vehicle or estradiol (E2, 167 ng per mouse per day) for 4 wk using slow-release pellets inserted s.c. (Innovative Research of America).

All mice were housed in a standard animal facility under controlled temperature (22 °C) and photoperiod (12 h of light, 12 h of dark) and the animal care was in accordance with institutional guidelines. All animal experiments had been approved by the local Ethical Committees for Animal Research at the University of Gothenburg.

Quantitative Real-Time PCR Analysis. Total RNA was prepared from humerus, middiaphyseal cortical bone of the tibia, vertebral body of vertebrae L_6 (trabecular bone) and uterus using TRIzol reagent (Life Technologies) followed by the RNeasy Mini Kit (Qiagen). The RNA was reverse transcribed into cDNA, and real-time PCR analysis was performed using predesigned real-time PCR assays for *Wnt16* (Mm00446420_m1), and osteoprotegerin (*Opg*; *Tnfrsf11b*, Mm0043545_m1) on the StepOnePlus Real-Time PCR system (Applied Biosystems). The mRNA abundance of each gene was adjusted for the expression of *18S*.

Dual-Energy X-Ray Absorptiometry (DXA). Analyses of total body areal BMD (aBMD) and lumbar spine (LS) BMD were performed by DXA using the Lunar PIXImus Mouse Densitometer (Wipro GE Healthcare).

High-Resolution Micro-CT (μCT). High-resolution micro-CT analyses were performed on the lumbar vertebra L_4 and tibia using an 1172 model micro-CT (Bruker micro-CT) (3). The vertebra and tibia were imaged with an X-ray tube voltage of 50 kV, a current of 201 μA, and with a 0.5-mm aluminum filter. The scanning angular rotation was 180°, and the angular increment was 0.70°. The voxel size was 4.49 mm isotropically. NRecon (version 1.6.9) was used to perform the reconstruction after the scans. In the vertebra, the trabecular bone in the vertebral body caudal of the pedicles was selected for analysis within a conforming volume of interest (cortical bone excluded) commencing at a distance of

4.5 μm caudal of the lower end of the pedicles, and extending a further longitudinal distance of 328 μm in the caudal direction. In the tibia, the trabecular bone distal to the proximal growth plate was selected for analyses within a conforming volume of interest (cortical bone excluded) commencing at a distance of 650 μm from the growth plate, and extending a further longitudinal distance of 134 μm in the distal direction. Cortical measurements were performed in the diaphyseal region of tibia starting at a distance of 5.2 mm from the growth plate and extending a further longitudinal distance of 134 μm in the distal direction.

Bone Histomorphometry. For the measurement of dynamic parameters, the mice were double labeled with calcein, which was injected (intraperitoneally) into the mice 1 and 8 d before termination. Femur and L_5 vertebrae were fixed in 4% paraformaldehyde, dehydrated in 70% EtOH and embedded in methyl methacrylate. Femur was dissected into two regions, one including proximal epiphysis and metaphysis and one including the cortical diaphyseal shaft. The distal femur and L_5 vertebrae were sectioned longitudinally, whereas the femur shaft was sectioned in a transverse plane. Static parameters were determined in a 4-μm-thick section stained in Masson–Goldner's Trichrome and dynamic parameters in an unstained 8-μm-thick section.

All parameters were analyzed using OsteoMeasure histomorphometry system (OsteoMetrics) following the guidelines of the American Society for Bone and Mineral Research (39). The analyses were performed by PharmaTest.

Mechanical Strength. Intact L_3 vertebrae were axially loaded after stabilizing them with a 1-mm-thick holder going through the vertebral foramen. The vertebral body was loaded with a press head of 2 mm in diameter. Loading speed were 0.155 mm/s using a mechanical testing machine (Instron 3366, Instron). Based on the computer recorded load deformation raw data curves produced by Bluehill 2 software v2.6 (Instron), the results were calculated with custom-made Excel macros.

Measurement of Serum Markers. As markers of bone resorption, serum levels of C-terminal type I collagen fragments were assessed using an ELISA RatLaps kit (CTX, Immunodiagostic Systems) according to the manufacturer's instructions and total amount of Trap5b was analyzed using a commercial TRACP 5b ELISA (Immunodiagostic Systems). Serum levels of osteocalcin (OCN), a marker of bone formation, were determined with a mouse osteocalcin immunoradiometric assay kit (Immutopics).

ACKNOWLEDGMENTS. We are grateful to A. Hansevi, B. Aleksic, and C. Uggla for technical assistance. This study was supported by the Swedish Research Council, the Swedish Foundation for Strategic Research, the ALF/LUA research grant from the Sahlgrenska University Hospital, the Lundberg Foundation, the Torsten and Ragnar Söderberg's Foundation, the Novo Nordisk Foundation, the Swedish Cancer Society, the Cancer Prevention and Research Institute of Texas (Grant RP110444-P1), the Texas Emerging Technology Fund under Agreement 18 No. 300-9-1958, and the Robert A. Welch Foundation (E-0004).

1. Khosla S, Melton LJ, 3rd, Riggs BL (2011) The unitary model for estrogen deficiency and the pathogenesis of osteoporosis: is a revision needed? *J Bone Miner Res* 26(3): 441–451.
2. Vandenput L, Ohlsson C (2009) Estrogens as regulators of bone health in men. *Nat Rev Endocrinol* 5(8):437–443.
3. Movérare-Skrtic S, et al. (2014) Osteoblast-derived WNT16 represses osteoclastogenesis and prevents cortical bone fragility fractures. *Nat Med* 20(11):1279–1288.
4. Zheng HF, et al. (2012) WNT16 influences bone mineral density, cortical bone thickness, bone strength, and osteoporotic fracture risk. *PLoS Genet* 8(7):e1002745.
5. Estrada K, et al. (2012) Genome-wide meta-analysis identifies 56 bone mineral density loci and reveals 14 loci associated with risk of fracture. *Nat Genet* 44(5):491–501.
6. Vanderschueren D, et al. (2014) Sex steroid actions in male bone. *Endocr Rev* 35(6): 906–960.
7. Daly E, et al. (1996) Risk of venous thromboembolism in users of hormone replacement therapy. *Lancet* 348(9033):977–980.
8. Anonymous; Collaborative Group on Hormonal Factors in Breast Cancer (1997) Breast cancer and hormone replacement therapy: Collaborative reanalysis of data from 51 epidemiological studies of 52,705 women with breast cancer and 108,411 women without breast cancer. *Lancet* 350(9084):1047–1059.
9. MacDonald BT, Tamai K, He X (2009) Wnt/beta-catenin signaling: Components, mechanisms, and diseases. *Dev Cell* 17(1):9–26.
10. Gong Y, et al.; Osteoporosis-Pseudoglioma Syndrome Collaborative Group (2001) LDL receptor-related protein 5 (LRP5) affects bone accrual and eye development. *Cell* 107(4):513–523.
11. Little RD, Recker RR, Johnson ML (2002) High bone density due to a mutation in LDL-receptor-related protein 5. *N Engl J Med* 347(12):943–944, author reply 943–944.
12. Little RD, et al. (2002) A mutation in the LDL receptor-related protein 5 gene results in the autosomal dominant high-bone-mass trait. *Am J Hum Genet* 70(1):11–19.
13. Boyden LM, et al. (2002) High bone density due to a mutation in LDL-receptor-related protein 5. *N Engl J Med* 346(20):1513–1521.
14. Poole KE, et al. (2005) Sclerostin is a delayed secreted product of osteocytes that inhibits bone formation. *FASEB J* 19(13):1842–1844.
15. Brunkow ME, et al. (2001) Bone dysplasia sclerosteosis results from loss of the SOST gene product, a novel cystine knot-containing protein. *Am J Hum Genet* 68(3): 577–589.
16. Balemans W, et al. (2002) Identification of a 52 kb deletion downstream of the SOST gene in patients with van Buchem disease. *J Med Genet* 39(2):91–97.
17. Loots GG, et al. (2005) Genomic deletion of a long-range bone enhancer misregulates sclerostin in Van Buchem disease. *Genome Res* 15(7):928–935.
18. Laine CM, et al. (2013) WNT1 mutations in early-onset osteoporosis and osteogenesis imperfecta. *N Engl J Med* 368(19):1809–1816.
19. Maeda K, et al. (2012) Wnt5a-Ror2 signaling between osteoblast-lineage cells and osteoclast precursors enhances osteoclastogenesis. *Nat Med* 18(3):405–412.
20. Bennett CN, et al. (2005) Regulation of osteoblastogenesis and bone mass by Wnt10b. *Proc Natl Acad Sci USA* 102(9):3324–3329.
21. Li X, et al. (2009) Sclerostin antibody treatment increases bone formation, bone mass, and bone strength in a rat model of postmenopausal osteoporosis. *J Bone Miner Res* 24(4):578–588.
22. Padhi D, Jang G, Stouch B, Fang L, Posvar E (2011) Single-dose, placebo-controlled, randomized study of AMG 785, a sclerostin monoclonal antibody. *J Bone Miner Res* 26(1):19–26.
23. Li X, et al. (2011) Dickkopf-1 regulates bone formation in young growing rodents and upon traumatic injury. *J Bone Miner Res* 26(11):2610–2621.
24. Gao Y, et al. (2013) Crosstalk between Wnt/β-catenin and estrogen receptor signaling synergistically promotes osteogenic differentiation of mesenchymal progenitor cells. *PLoS One* 8(12):e82436.
25. Kouzmenko AP, et al. (2004) Wnt/beta-catenin and estrogen signaling converge in vivo. *J Biol Chem* 279(39):40255–40258.
26. Armstrong VJ, et al. (2007) Wnt/beta-catenin signaling is a component of osteoblastic bone cell early responses to load-bearing and requires estrogen receptor alpha. *J Biol Chem* 282(28):20715–20727.
27. Zhang QG, Wang R, Khan M, Mahesh V, Brann DW (2008) Role of Dickkopf-1, an antagonist of the Wnt/beta-catenin signaling pathway, in estrogen-induced neuroprotection and attenuation of tau phosphorylation. *J Neurosci* 28(34):8430–8441.
28. Hou X, Tan Y, Li M, Dey SK, Das SK (2004) Canonical Wnt signaling is critical to estrogen-mediated uterine growth. *Mol Endocrinol* 18(12):3035–3049.
29. Lim SK, Orhant-Prioux M, Toy W, Tan KY, Lim YP (2011) Tyrosine phosphorylation of transcriptional coactivator WW-domain binding protein 2 regulates estrogen receptor α function in breast cancer via the Wnt pathway. *FASEB J* 25(9):3004–3018.
30. Medina-Gomez C, et al. (2012) Meta-analysis of genome-wide scans for total body BMD in children and adults reveals allelic heterogeneity and age-specific effects at the WNT16 locus. *PLoS Genet* 8(7):e1002718.
31. Koller DL, et al. (2013) Meta-analysis of genome-wide studies identifies WNT16 and ESR1 SNPs associated with bone mineral density in premenopausal women. *J Bone Miner Res* 28(3):547–558.
32. García-Ibarbia C, et al. (2013) Missense polymorphisms of the WNT16 gene are associated with bone mass, hip geometry and fractures. *Osteoporos Int* 24(9):2449–2454.
33. Hendrickx G, et al. (2014) Variation in the Kozak sequence of WNT16 results in an increased translation and is associated with osteoporosis related parameters. *Bone* 59:57–65.
34. Wergedal JE, Kesavan C, Brommage R, Das S, Mohan S (2015) Role of WNT16 in the regulation of periosteal bone formation in female mice. *Endocrinology* 156(3): 1023–1032.
35. Clevers H, Loh KM, Nusse R (2014) Stem cell signaling. An integral program for tissue renewal and regeneration: Wnt signaling and stem cell control. *Science* 346(6205): 1248012.
36. Willert K, et al. (2003) Wnt proteins are lipid-modified and can act as stem cell growth factors. *Nature* 423(6938):448–452.
37. Turner RT (1999) Mice, estrogen, and postmenopausal osteoporosis. *J Bone Miner Res* 14(2):187–191.
38. Windahl SH, Vidal O, Andersson G, Gustafsson JA, Ohlsson C (1999) Increased cortical bone mineral content but unchanged trabecular bone mineral density in female ERbeta(-/-) mice. *J Clin Invest* 104(7):895–901.
39. Dempster DW, et al. (2013) Standardized nomenclature, symbols, and units for bone histomorphometry: A 2012 update of the report of the ASBMR Histomorphometry Nomenclature Committee. *J Bone Miner Res* 28(1):2–17.